

# Adsorption of Alizarin, Eriochrome Blue Black R, and Fluorescein Using Different Iron Oxides as Adsorbents

Silvina Pirillo,<sup>†</sup> María Luján Ferreira,<sup>†,‡</sup> and Elsa H. Rueda<sup>\*,†</sup>

Departamento de Química, Universidad Nacional del Sur, Avenida Alem 1253, B8000CPB Bahía Blanca, Argentina, and Planta Piloto de Ingeniería Química (PLAPIQUI-UNS-CONICET) Camino a la Carrindanga km 7, B8000CPB Bahía Blanca, Argentina

This work presents kinetic and thermodynamic analysis of the adsorption of three dyes: alizarin, eriochrome blue black R, and fluorescein onto goethite, Co-goethite, and magnetite of medium Brunauer–Emmett–Teller surface area. The adsorption of the dyes on the oxides is fast. Fluorescein exhibits the lowest level adsorption for all adsorbents with goethite being the most efficient adsorbent when milligrams of dye per gram of oxide are considered. The Langmuir isotherm is the most appropriate for describing the adsorption data for the following systems: alizarin–magnetite and eriochrome and fluorescein with the three adsorbents, while alizarin–goethite and alizarin–Co-goethite show better fits with Freundlich isotherm. Molecular modeling using MM2 was used to analyze the steric effects on adsorption.

## 1. Introduction

Color removal from textile effluents has been the target of great attention in the past few years, not only because of the colors' potential toxicity but mainly due to visibility problems.<sup>1,2</sup> Recent estimates indicate that approximately 12% of synthetic textile dyes used each year are lost during manufacture and processing operations and 20% of these lost dyes enter the environment through effluents derived from the treatment of industrial wastewaters.<sup>3,4</sup> Effluents discharged from dyeing industries are highly colored, and they can be toxic to the aquatic life in receiving waters.<sup>5–7</sup>

Although conventional chemical<sup>8–10</sup> and biological<sup>11–13</sup> treatments have been applied for the removal of dyes from textile wastewater, these processes are insufficient in removing dye contaminants since dyes are stable to light, heat, and oxidizing agents.<sup>14</sup> Since individual technique is not sufficient to achieve complete decolorization, efficient strategies for dye removal consist of a combination of different techniques.

Adsorption has evolved into one of the most effective physical processes for decolorization of the textile wastewaters since it can produce high-quality water and also be a process that is economically feasible.<sup>15</sup> The most commonly used adsorbent for color removal is activated carbon, because of its capability for efficiently adsorbing a broad range of different types of adsorbates.<sup>16</sup> However, due to the problem of activated carbon's cost, the use of alternative adsorbents is attractive. Several researchers have been studying the use of other materials, which, although less efficient, involve lower costs.<sup>17</sup> The use of synthetic iron oxides is much more economical than commercial highly efficient, activated carbon, in a 30:1 relative ratio—depending on the particular kind of activated carbon.

Iron oxides, oxyhydroxides, and hydroxides are important constituents of many natural and engineered environmental systems. Due to their reactive surfaces and large specific surface areas, iron oxides can exert strong controls on overall system biogeochemistry through abiotic and biotic processes. The

transformation of organic and inorganic contaminants at the iron oxide–water interface is particularly important in the design and management of treatment and remediation technologies. It is well-known that iron oxides sequester cations and radionuclides, are strong adsorbents of anions such as arsenate, chromate, and phosphate and pesticides, humic or fulvic acids.<sup>18</sup> The adsorption ability of the iron oxides arises from the surface hydroxyl group's intervention during dissociative chemisorption of the adsorbate. Goethite has been the iron oxide most studied because of its high thermodynamic stability. Substituted goethites are interesting due to their adsorption properties, able to be modified by the presence of a foreign ion. In this way, Co-goethite has been selected in this study. Finally, the magnetic properties of magnetite particles allow the fast magnetic separation of metal ions from industrial effluent and nuclear waste stream.

However, there are still many unanswered questions about processes in the iron oxides systems. Particle aggregation is common; behaviors in the uptake and release of adsorbates are not simple. Many times, only a fraction of the initially adsorbed species is released to the solution, and the consideration is that the adsorbate has been “irreversibly adsorbed”. Possibilities of precipitation as a separate phase, cluster formation, inclusions in the structures, and the role of partial dissolution have been proposed as potential effects. Because dissolution is not the reverse of precipitation in the case of these oxides, which it is not in other cases, the molecular effects at surface are important to take into account. Even more, the structure we are interested in is the microporous one, because the mesoporous structures many times are related to interparticle separation due to the particle size of iron oxides.<sup>18</sup>

In the case of goethite, the morphology is closely related to the BET area.<sup>19</sup> Crystal lengths of synthetic goethites of 60–70 m<sup>2</sup>/g were reported to be near 1  $\mu$ m. When goethite presents BET areas higher than 50 m<sup>2</sup>/g, the morphology is in needles with the (110) faces corresponding to the sides, whereas the (021) corresponds to the ends. In general, goethite has been characterized in pore size using adsorption/desorption N<sub>2</sub> isotherms and (i) Brunauer–Emmett–Teller (BET) areas, (ii) the Barrett–Joyner–Halenda (BJH) method for mesoporous size distribution, (iii) micropore size distribution with the Horvath–Kawazoe (HK) method, and (iv) the area external to the

\* To whom correspondence should be addressed. Tel.: (+54) 291-4595159. Fax: (+54) 291-4595160. E-mail address erueda@uns.edu.ar.

<sup>†</sup> Universidad Nacional del Sur.

<sup>‡</sup> PLAPIQUI-UNS-CONICET.

micropores using the *t*-plot methods. Generally, goethite of 37–40 m<sup>2</sup>/g presents micropores—by HK method—in the range of 8–9 Å and mesopores—by the BJH method—in the 20–300 Å range and a content of external micropores not higher than 2%. In the case of higher BET areas of goethites—near 90 m<sup>2</sup>/g—the micropore size is similar to the one obtained with lower BET areas of goethites—near 8–9 Å—but the external micropore area obtained with the *t*-plot method achieves the 6–7% range and the mesopores size distribution is bimodal.<sup>20</sup> The surface complexes of phthalate, trimellitate, and pyromellitate were described as inner sphere complexes at pH lower than 6 and outer sphere complexes at pH 6–9. Discrepancies between charging curves cannot be assigned to differences in the BET area and roughness is considered an important variable to take into account. There are several published manuscripts on the variability of the reported adsorption sites on goethite.<sup>21,22</sup>

In the case of magnetite, surface properties have been studied carefully.<sup>23</sup> Magnetite can transform to maghemite and release ferrous ions at acidic pHs. It has been shown by scanning electron microscopy/transmission electron microscopy (SEM/TEM) that synthetic magnetite particles are mainly aggregates. The size of the magnetite particles achieves values lower than 150 Å, on average, for the main fraction in weight. The specific surface area has been reported to be near 96 m<sup>2</sup>/g, using the equation  $S = 3/(\text{sample density} \times \text{particle ratio})$  considering a sample density of 5.2 g/cm<sup>3</sup> and a particle ratio of  $6 \times 10^{-7}$  cm. Mossbauer studies have confirmed the micro to nano character of the synthetic magnetite. Comparisons with goethite in terms of sorption<sup>24</sup> were modeled using the Temkin isotherm. To consider the BET area as a parameter to select the experimental conditions in adsorption of organic molecules from aqueous solution is a reported procedure. Considering the reported percentage of microporosity in the samples of goethite and magnetite—not more than 6%—and then BET areas found, these results are in line with the reported idea of the quantification of an external area of the particles due to the particle size of the oxides. The external surface area would be close to the measured BET areas. Because of the measurement in solid of the BET areas, it is probable that particle aggregates give rise to mesoporous and particular mesoporous structures in goethite and magnetite.<sup>25</sup>

In this work the ability of three different adsorbents, goethite, Co-substituted goethite, and magnetite, to remove dyes with azo, anthraquinone, and aril–methane groups (alizarin, eriochrome blue black R, and fluorescein) have been studied using the adsorption isotherms and kinetic analysis. These dyes were chosen because of their structures, which are commonly present in dyes of the textile industry. The experimental results were fitted into Langmuir and Freundlich equations, considered the most adequate adsorption isotherms for dyes adsorption after the literature revision. Molecular mechanics methods were also employed to study the steric interactions of dye–oxide surfaces for a better understanding of the adsorption process.

## 2. Experimental Section

**2.1. Materials.** **2.1.1. Adsorbents.** The three adsorbents used in this investigation, goethite, Co-goethite, and magnetite, were prepared in our laboratory.

**2.1.1.1. Goethite** was prepared by adding aqueous Fe(NO<sub>3</sub>)<sub>3</sub>·9H<sub>2</sub>O (0.05 mol) to NaOH (2.5 mol/L) to reach a 1.5 OH:Fe ratio, in a final volume of 100 mL. The precipitate was aged at room temperature for 48 h and then in a vacuum oven at 65 °C for 72 h.

**2.1.1.2. Co-goethite** was prepared by adding aqueous NaOH (175 mL, 2 mol/L) to a solution (50 mL,  $2.65 \times 10^{-3}$  mol of

**Table 1. Surface Area, Pore Volume, and Pore Size for Iron Oxides Goethite, Co-goethite, and Magnetite**

property	goethite	Co-goethite	magnetite
surface area (m <sup>2</sup> /g), multipoint BET	69	56	42
pore volume (cm <sup>3</sup> /g), HK method cumulative pore volume	0.027	0.023	0.017
pore size (Å), HK method pore radius (micropores)	9.7	7.7	7.8
pore size (Å), BJH method pore radius (mesopores)	55	15	100

Co and 0.02385 mol of Fe). Then, the precipitate was washed, centrifuged, and placed in NaOH (250 mL, 0.3 mol/L). After that, it was aged in a vacuum oven at 60 °C for 10 days.

**2.1.1.3. Magnetite** was prepared by adding FeSO<sub>4</sub>·7H<sub>2</sub>O (250 mL, 0.53 mol/L) at a constant rate (2.8 cm<sup>3</sup>/min) to 300 mL of a solution containing 0.35 mol of NaOH and 0.05 mol of NaNO<sub>3</sub> under vigorous stirring. The sample was aged at room temperature for 16 days.

All samples were washed up to raise the conductivity of doubly distilled water. Then, they were dried at 40 °C for 72 h before use. The surface areas and porosity of the three oxides are presented in Table 1. The specific surface area of the samples was measured by the classical Brunauer–Elmet–Teller method using a multiple point adsorption nitrogen process (BET-N<sub>2</sub>) with a Quantachrome Nova 1200e instrument, with software appropriate for the application of the BJH and HK methods.

X-ray diffraction (XRD) patterns indicate a unique phase for goethite and Co-goethite, but the presence of goethite as a minor phase is registered in magnetite (results not shown).<sup>26–28</sup>

**2.1.2. Adsorbates.** Three different commercially available textile dyes were used in the study: (1) alizarin (anthraquinone dye), with  $\lambda_{\text{max}} = 531$  nm; (2) eriochrome blue black R (azo dye), with  $\lambda_{\text{max}} = 527$  nm; and (3) fluorescein (triarylmethane dye) with a  $\lambda_{\text{max}} = 491$  nm. Chemical structures are shown in Figure 1. All reagents used in this study were of an analytical grade.

The  $pK_a$  of the different groups are the following: (a) Eriochrome blue black R,  $pK_1$  H2L/HL.H, 7.31;  $pK_2$  HL/HL, 13.8.<sup>29</sup> (b) Fluorescein,  $pK_1$  H3L/H2L.H, 2.27;  $pK_2$  H2L/HL.H, 4.32;  $pK_3$  HL/H.L, 6.50.<sup>30</sup> (c) Alizarin,  $pK_1$  H2L/HL.H, 5.25;  $pK_2$  HL/H.L, 11.5.<sup>31</sup>

**2.2. Methods.** The effect of contact time and adsorbate dosage on color removal was studied in a series of kinetic and equilibrium experiments. The experiments were carried out with a background concentration of 0.05 M NaCl to maintain a constant ionic strength.

**2.2.1. Kinetic Experiments.** In each kinetic experiment, a known quantity of adsorbent was contacted with 100 mL of the dye solution with predetermined initial dye concentration, in a thermostatic shaker bath at room temperature for a given recorder time (0.15, 0.30, 0.45, 0.60, 0.90, 1.20, or 1.80 h). The initial pH of the solutions was adjusted to  $7.10 \pm 0.1$  by the addition of diluted solutions of either sodium hydroxide or hydrochloric acid. The initial concentration of adsorbent was 100 mg/L for goethite and Co-goethite and 200 mg/L for magnetite. A 25 mg/L amount of dye was used in all experiences. After a specified stirring time period, the reaction mixture was vacuum filtered and the pH of the filtrate was measured. Due to the BET area, the pore volume, and the pore size of magnetite, we used a larger amount of this oxide.

The amount of dyes adsorbed was determined by the difference between the initial and final concentrations measured spectrophotometrically with a Cecil UV–vis spectrophotometer.

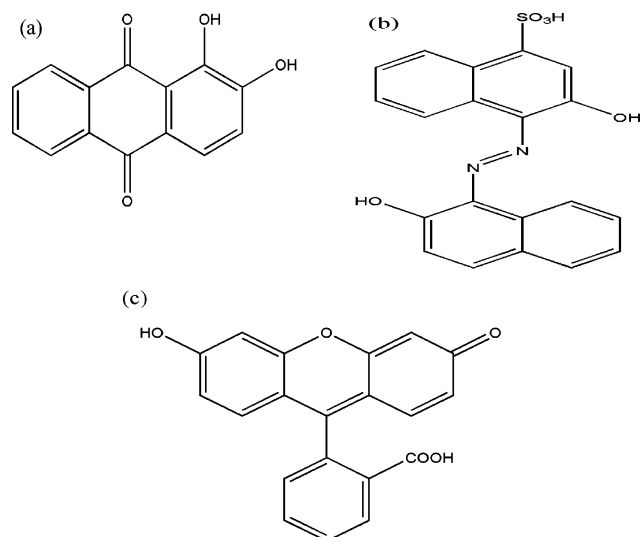


**Figure 1.** Structures of the dyes used: (a) alizarin; (b) eriochrome blue black R; (c) fluorescein.

These experiments were used to establish the equilibrium time between the adsorbents and the dye solutions. Additional studies performed at various initial dye concentrations indicated that the adsorption occurred very quickly within the first 90 min.

**2.2.2. Equilibrium Experiments.** In these experiences the adsorbent was added to different quantities of dye solutions into 250 mL flasks and subsequently placed on a shaker for 2 h at room temperature. The magnetite concentration was 2 g/L, and goethite and Co-goethite concentrations were 1 g/L. The contact time was chosen to ensure a maximum adsorption capacity. A range between 15 and 120 mg/L of initial dye solution was employed in all cases. After equilibrium, each withdrawn sample was filtrated with a 0.45  $\mu\text{m}$  membrane filter to remove the solid particles. The filters we used were composed of modified pure cellulose acetate. The adsorbed amounts were determined by the difference between initial and final concentration and expressed as milligrams of dye per gram of adsorbent. In each case, duplicate blank experiments were also conducted.

**2.2.3. Dye Concentration Measurement and Calibration.** To calculate the concentration of the sample from each experiment, a calibration curve of each dye was first performed. The absorbance values of each dye, before and after treatment, were measured at their respective maximum wavelengths.

**2.3. Theoretical Studies. 2.3.1. The Program.** The software MM2 from the Package included in ChemBats3D ultra5.0 from Cambridge Soft was used to model the goethite and magnetite surface. The goal was to test steric effects; therefore, electronic characteristics were not included in the parametrization.

The steric energy is presented as the summation of bond stretching, bond-angle bending, torsion angle deformations, and nonbonded interaction energies along with other relevant terms. It is an empirical number that does not account for electronic interactions, but it can provide approximately ion-ion interactions and dipole-dipole interactions. Only different conformations with the same atom number and different atom distributions—with no broken bonds, but conformationally different—can be compared, using the same force field and the same number and kind of bonds involved. There are a lot of reports about the use of molecular mechanics in the study of steric interactions, even in transition metal complexes and oxides, where the importance of electronic effects is known.<sup>32–34</sup>

**2.3.2. Surface Models.** Goethite is usually described using the *Pbnm* group. The structure consists of double rows or

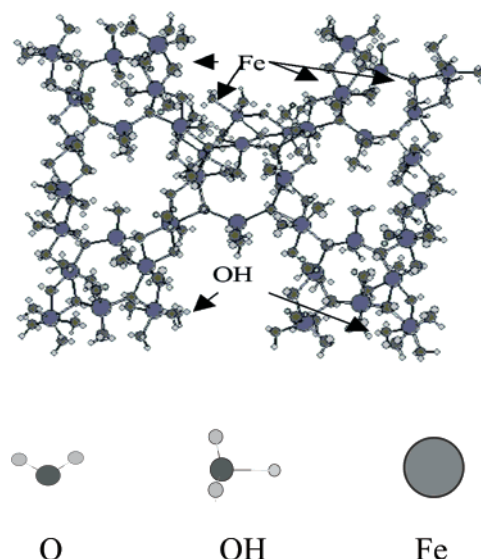


**Figure 2.** Magnetite (111) face. The O and OH include the lone pair on oxygen.

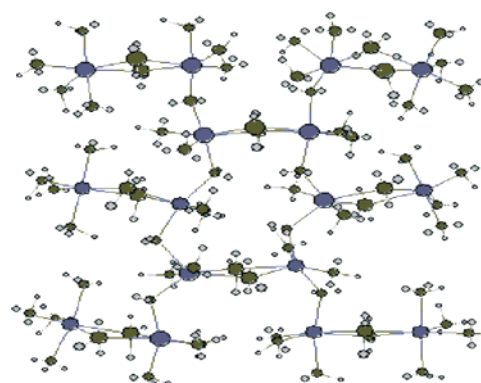


**Figure 3.** Goethite projected on (001). Anionic packing showing the hcp of anions. Lone pair shown in oxygen.

ribbons of edge-sharing Fe octahedral that run parallel to [001]; these double rows are separated by vacant double rows of channels that also run along [001]. The double rows are formed by polyhedral that share two hydroxide groups. The ribbons along [001] are formed by the connection of polyhedral that share one oxide and one hydroxide group from the same edge.<sup>35</sup>

Magnetite has the spinel ( $\text{MgAl}_2\text{O}_4$ ) structure, with a cubic close packed oxygen array, and iron in both 4-fold and 6-fold coordination; magnetite is frequently observed in nature as octahedral crystals exhibiting {111} faces. Magnetite has the cubic *Fd3m* space group.<sup>23</sup>

Figures 2 and 3 show the steric views of the surface of goethite and magnetite preferred planes.

**2.3.3. Dyes Models.** On the surface models of goethite calculations of parallel and perpendicular adsorption forms of the dyes were included. All the dyes were modeled as neutral molecules and ionized ones when possible, considering the parametrization available: O as carboxylate in the case of fluorescein and O from sulfonic ionized group in the case of eriochrome blue black R.

### 3. Results and Discussion

#### 3.1. Kinetic Experiments with Aqueous Dye Solutions.

Figure 4 shows the amount of adsorbed dye as a function of contact time, on the different adsorbents.

Under the experimental conditions alizarin onto goethite reaches the maximum adsorption in a few minutes, indicating

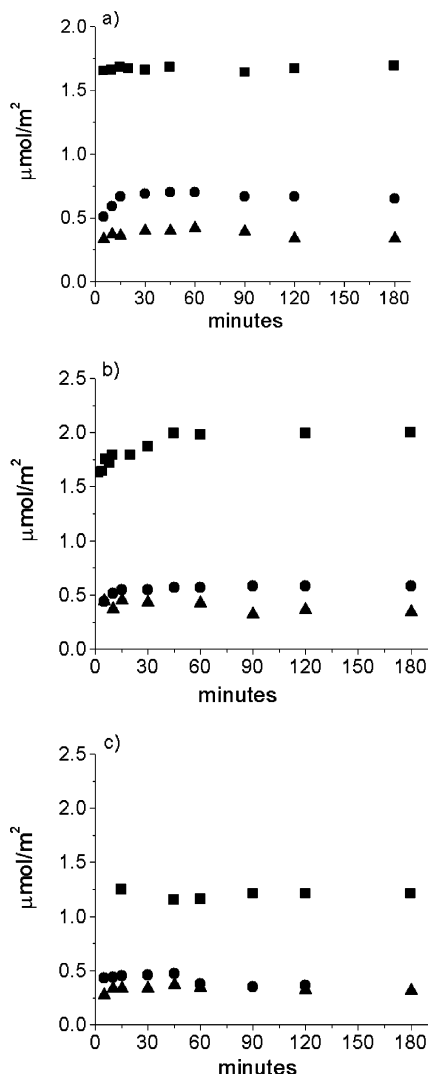


**Figure 4.** Dyes removal as function of time by the three examined adsorbents: (a) goethite; (b) Co-goethite; (c) magnetite. (■) Alizarin; (●) eriochrome blue black R; (▲) fluorescein.

high affinity between adsorbent and dye. When the adsorbent is Co-goethite, alizarin adsorption is also a fast process but the equilibrium is reached after about 1 h of contact. This behavior is also found in the adsorption rate of Alizarin onto magnetite. A comparison among different supports indicated a higher adsorption of alizarin onto Co-goethite; however, when the adsorbed amount is expressed in milligrams of adsorbate per gram of oxide, goethite shows the highest adsorption level.

A fast adsorption is also found for eriochrome blue black R onto the different adsorbents with similar adsorption levels for the three adsorbents. However, when these results are expressed in milligrams of adsorbate per gram of oxide, the following sequence is observed: goethite > Co-goethite > magnetite. Fluorescein exhibits the lowest level adsorption for all adsorbents, with the goethite being the most efficient when milligrams of dye per gram of oxide are considered. The equilibrium is reached at longer periods, as if a rearrangement of the dye's molecules on the surface is taking place.

**3.2. Adsorption Isotherm Experiments with Aqueous Dye Solutions.** The adsorption isotherms describe how adsorbates interact with adsorbents and are critical in the optimizing of the use of adsorbents. It is generally possible to express the results of the experimental sorption measurements as equilibrium sorption isotherms. In this study, two types of isotherms have

been investigated, namely, Langmuir and Freundlich isotherm. The sorption process is then discussed in terms of constants, which are characteristic for the individual systems. The Langmuir equation assumes that there is no interaction between the adsorbate molecules and that the sorption is localized in a monolayer. The enthalpy of adsorption is independent of surface coverage. It is then assumed that once a dye molecule occupies a site, no further sorption can take place at that site. Theoretically, therefore, a saturation value is reached, beyond which no further sorption can take place. The Freundlich equation is an empirical relationship describing the sorption of solutes from a liquid to a solid surface. It describes heterogeneous adsorption and is not restricted to the formation of the monolayer.

### 3.2.1. Langmuir Isotherm.

$$n_z^s = (n^s K_L C_{eq}) / (1 + K_L C_{eq}) \quad (1)$$

where “ $n^s$ ” is the number of adsorption sites, “ $K_L$ ” is the equilibrium constant for dye adsorption, and “ $n_z^s$ ” represents the limiting number of dye moles that can be adsorbed onto a gram of oxide.

**3.2.2. Freundlich Isotherm.** This isotherm assumes a logarithmic fall in the enthalpy of adsorption with surface coverage:

$$q_e = K_F C_e^{1/n} \quad (2)$$

where  $C_e$  is the equilibrium concentration of dyes in solution ( $\mu\text{mol}/\text{L}$ ),  $q_e$  indicates solid-phase sorbate concentration at equilibrium ( $\mu\text{mol}/\text{m}^2$ ), and  $K_F$  is the Freundlich constant (the larger this value is, the higher the capacity), and  $1/n$  is a heterogeneity coefficient. Higher values of this coefficient mean lesser heterogeneity.

To decide which type of isotherm fits better the sorption experimental data, a no linear curve fit from Origin 5.0 Professional was used. The  $\chi^2$  test was used as a criterion for the quality of fitting. In this test, the squared difference between the experimental data and calculated data is divided by the calculated data obtained from the model. The value of  $\chi^2$  is used to evaluate the fit of the isotherm to experimental data, whereas the smaller the  $\chi^2$ , the better is the fit. Figure 5 shows the experimental data fitted with Langmuir isotherm and Figure 6 the fittings with Freundlich isotherm.

All isotherms can be described by Langmuir and Freundlich equations.

On the basis of  $\chi^2$  values and the standard errors of parameters, the Langmuir isotherm is the most appropriate for describing adsorption data for the following systems: alizarin–magnetite, eriochrome blue black R, and fluorescein with the three adsorbents, while alizarin–goethite and alizarin–Co-goethite show better fits with Freundlich isotherm.

**3.3. Efficiency of Adsorption.** Figure 7 shows that in the experimental conditions employed in this work the following sequence in the efficiency of removing is obtained: alizarin > eriochrome blue black R > fluorescein.

The color removal efficiency was found to be as high as 90% for alizarin onto goethite and Co-goethite, whereas levels of 90–70% of removal were reached for eriochrome blue black R on goethite and 80–70% on Co-goethite. Fluorescein is the dye that exhibits the least interaction with the adsorbents studied, with a maximum removal of 30%. A comparison among the efficiency of goethite and Co-goethite shows similar results, while a lesser efficiency is observed for magnetite.

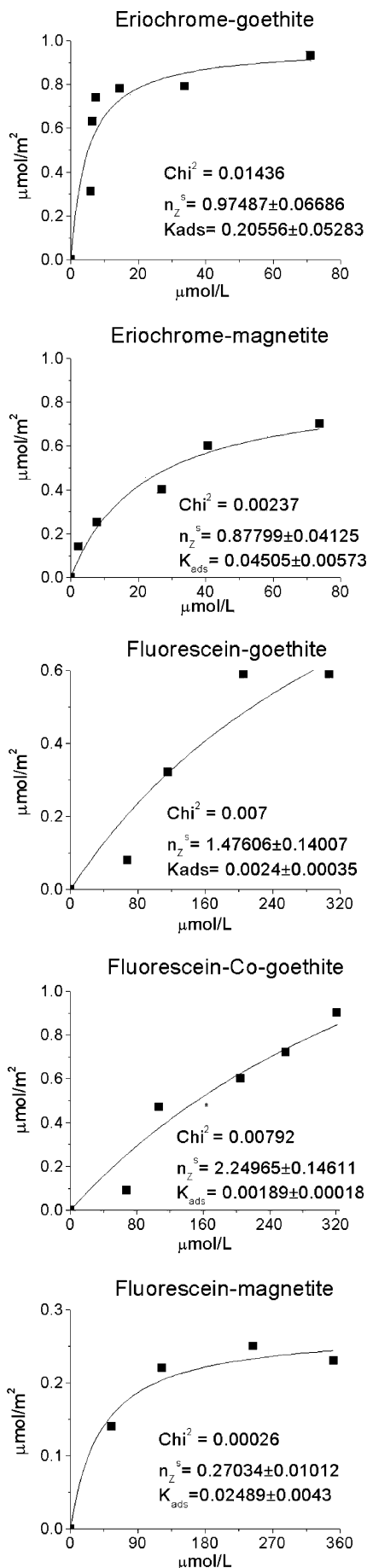


**Figure 5.** Langmuir isotherms: (■) experimental data; (—) fit from Langmuir equation.  $n_z^s$  units:  $\mu\text{mol}/\text{m}^2$  oxide.  $K_L$  units:  $\text{L}/\mu\text{mol}$ .

The adsorption maximum uptake obtained from Langmuir isotherm reported for methylene blue (MW = 337.85 g/mol) on activated carbon was  $0.284 \mu\text{mol}/\text{m}^2$ .<sup>36</sup> In this work the adsorption capacity for fluorescein (MW = 332.32 g/mol) on magnetite was  $0.2703 \mu\text{mol}/\text{m}^2$ . The similarity between these values for two dyes with similar molecular weight show that the adsorption maximum uptake for both activated carbon and magnetite are comparable when the adsorption results are expressed as the mass of dye adsorbed per area unit. Values of  $n_z^s$  obtained for goethite and Co-goethite are still higher. Therefore, the iron oxides studied are as effective adsorbents as carbon, but with a specific area smaller than the activated carbon.

**3.4. Theoretical Results.** In the case of magnetite Table 2 shows that perpendicular alizarin and eriochrome blue black R (namely, a) adsorption is preferred to parallel adsorption (namely, b).

In the case of alizarin the decrease in steric energy ( $\Delta\text{SE}$ ) upon adsorption is near  $-45$  kcal/mol. In the case of ionized eriochrome blue black R the energy achieves values as high as  $-560$  to  $-600$  kcal/mol. For ionized fluorescein the decrease in the steric energy is near  $-455$  kcal/mol and in the case of molecular fluorescein is between  $-35$  and  $-70$  kcal/mol, depending on the conformation on the surface.

Figure 8 shows adsorption of alizarin and eriochrome blue black R onto magnetite.

On the basis of the conformation found on magnetite, we can calculate a projection of the molecule on the exposed surface. Alizarin occupies a surface of  $36 \text{ \AA}^2$  (based on two alizarin on magnetite complete; see Figure 8a), fluorescein  $114 \text{ \AA}^2$  (results not shown), and eriochrome blue black R  $119 \text{ \AA}^2$  (see Figure 8b). Therefore the differences are not related to the occupied surface.

On magnetite, adsorption of two eriochrome blue black R and fluorescein molecules close to each other are more favorable than the adsorption of two alizarin molecules close to each other (results not shown). In this case, there are alternative forces that must be considered to explain the trends obtained in dye adsorption, even when steric interactions are well-considered. In the same way, geometric considerations about the particle size, surface sites distribution, and electrostatic/electronic effects are important to understand the overall tendency.

Adsorption onto goethite shows definite trends. Fluorescein and eriochrome blue black R show similar changes in steric energies, whereas alizarin shows lower changes in steric energies upon adsorption (see Table 2). Figure 9 shows different views of alizarin, eriochrome blue black R, and fluorescein onto goethite.

Calculations including a second complete molecule of dye were performed on the two surfaces. In the case of goethite, the trend followed that experimentally found, being the adsorption of two alizarin molecules close to each other more favorable than the adsorption of two eriochrome blue black R close to each other and the previous more favorable than two fluorescein ( $-12$ ,  $38$ , and  $59$  kcal/mol).

Eriochrome blue black R can be adsorbed in perpendicular form 1, with only one point of contact, the  $\text{SO}_3^-$  group, or in perpendicular form 2, where the negative charges can be far away one from the other if we consider the negative charge of the  $\text{SO}_3^-$  group. The increase of the dye concentration probably changes the relation between perpendicular form 1, which is considered to show a projected area of  $119 \text{ \AA}^2$ , to a perpendicular form 2, which occupies near  $161 \text{ \AA}^2$  with some interactions of OH groups of eriochrome blue black R with the

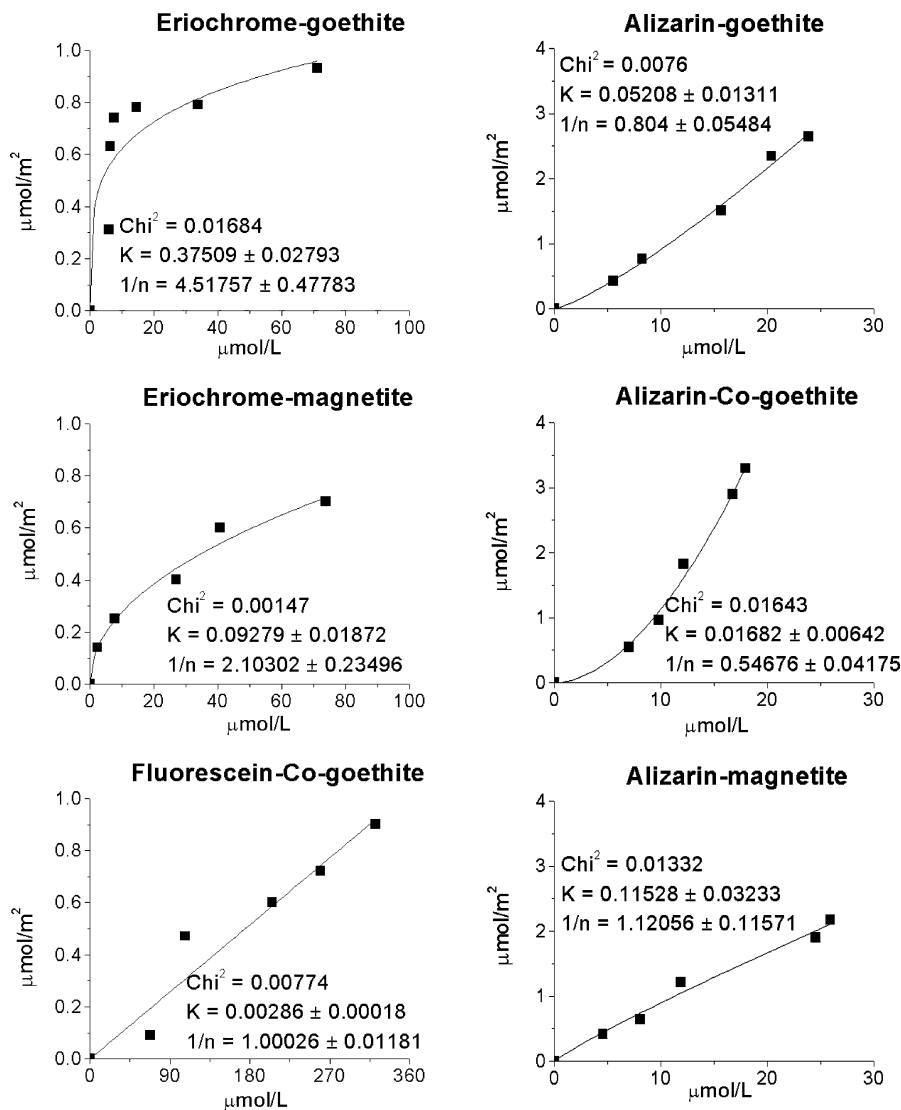


Figure 6. Freundlich isotherms: (■) experimental data; (—) fit from Freundlich equation.

surface. This geometrical consideration could partially explain the decrease of the uptake in the case of Co-goethite and magnetite versus goethite, considering also the surface structural changes that Co induces in goethite and the presence of Fe<sup>2+</sup>/Fe<sup>3+</sup> on the surface of magnetite.

Surfaces may have different reactivities due to the variations in the coordination of oxide surface functional groups comprising the surface or anisotropic surface dielectric properties or from the influence of interfacial solvent structure. The pattern of charge development influences the thermodynamics and kinetics of acid–base, surface complexation, and oxidation–reduction reactions in these systems. In goethite the (021) surface plane presents a higher density of singly coordinated ≡FeOH surface functional groups (8.2 FeOH sites/nm<sup>2</sup>), while the (110) surface has 3.0 ≡FeOH sites/nm<sup>2</sup>. On the other hand, the octahedral (111) face of magnetite contains singly and doubly coordinated hydroxides. The site density of the magnetite (111) face is 5.47 μmol/m<sup>2</sup> (6.11 μmol/m<sup>2</sup> for γ-corundum), where the total hydroxide content is doubly coordinated.

Different types of edges present vary significantly in their Brønsted acidity. It is not only the ability of the water to solvate the positively charge surface functional group, but also the ability of the water to solvate the associated OH counterion which determines the surface charge distribution.

Considering alizarin, fluorescein, and eriochrome blue black R, near the surface, we can consider the following: (1) alizarin with two ionized OH<sup>−</sup> and two O<sup>−</sup> near one another (see Figure 1); (2) eriochrome blue black R with the sulfonic ionized and two OH (these probably are not ionized); (3) fluorescein with one carboxylate anion and one OH (non-ionized).

Therefore we are comparing an adsorbed molecule almost surely molecularly ionized at surface (but not in solution; therefore, the adsorption step is important), and two ionized molecules—from solution—such as eriochrome blue black R (ionized sulfonic group) and fluorescein (ionized carboxylate group).

To stabilize charges, we need specific sites ≡FeOH<sub>2</sub><sup>+</sup> on the surface and the displacement of the OH<sup>−</sup> by the anion, with the maintenance of overall neutrality by compensation.

In the case of alizarin, one surface site can stabilize one OH<sup>−</sup> ionized and the adsorption will be strong. The planar nature of the molecule makes it without any hindrance to adsorb.

In the case of eriochrome blue black R, the sulfonic is strong enough to be coordinated, whereas the OH with pK<sub>a</sub> 13.8 can remain non-ionized. Fluorescein seems to be interacting through the carboxylate ion and/or the ionized OH, in the same situation as the case of eriochrome blue black R. However, the molecule

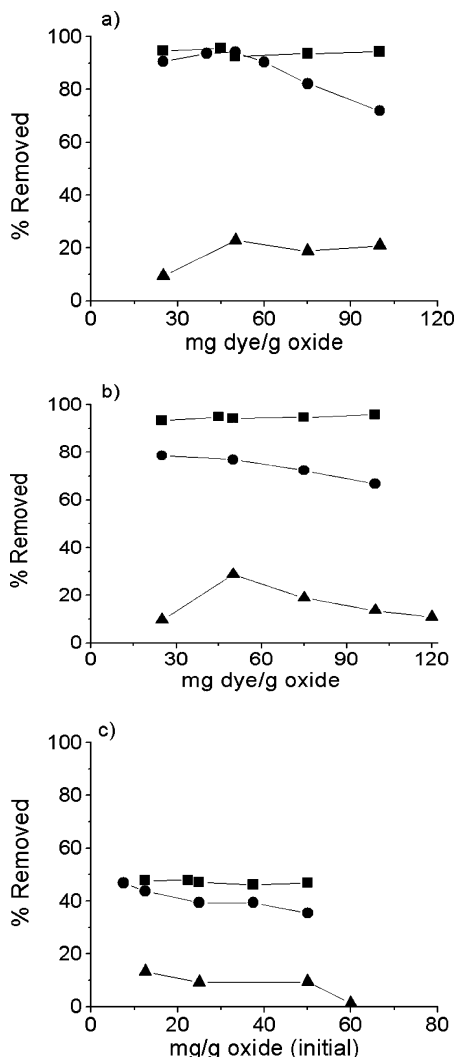


**Figure 7.** Percentage of dye removed as a function of milligrams of dye per gram of oxide initial ratio: (a) goethite; (b) Co-goethite; (c) magnetite. (■) Alizarin; (●) eriochrome blue black R; (▲) fluorescein.

**Table 2. Results of MM2 Calculation Applied to the Interaction of the Dye with Magnetite or Goethite**

dye	steric energy <sup>a</sup>	$\Delta SE^{a,b}$
(1) alizarin a-goethite	1748.1	-20.6
(2) alizarin b-goethite	1730	-36.9
(3) fluorescein a-goethite	1724.4	-41.5
(4) fluorescein b-goethite	1733.5	-34.4
(5) fluorescein ionized-goethite	1687.5	-73.6
(6) eriochrome a-goethite	1619.4	-40.3
(7) eriochrome b-goethite	1631.4	-29.8
(8) alizarin a-magnetite	7447.6	-45.7
(9) alizarin b-magnetite	7449.1	-44.2
(10) fluorescein a-magnetite	7423.8	-70.3
(11) fluorescein b-magnetite	7461.8	-32.3
(12) fluorescein ionized-magnetite	7010.8	-455.2
(13) eriochrome a-magnetite	6797	-562.3
(14) eriochrome b-magnetite	7456.5	-3.7
(15) ionized eriochrome b-magnetite	6765.4	-593.9
(16) molecular eriochrome	7385.4	-77.7

<sup>a</sup> Unit of steric energy and  $\Delta SE$  is kilocalories per mole (kcal/mol). <sup>b</sup>  $\Delta SE$  is the change of the steric energy of the completely separated dye and goethite vs the coordinated dye on the goethite.

must be twisted to be adsorbed in the case of fluorescein, and there is no possibility of perpendicular adsorption. The difference for fluorescein is not related to the surface, but to the compound itself. The combination of the twisting that is necessary for the molecule to be adsorbed and the  $K_a$  of the

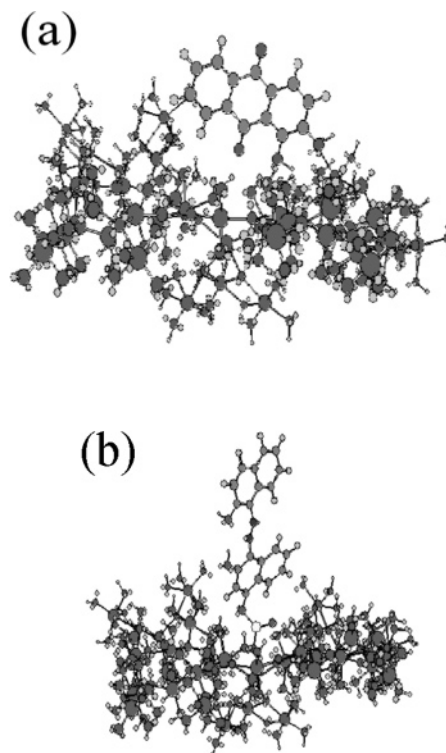


**Figure 8.** Adsorption onto magnetite, lateral view: (a) alizarin; (b) eriochrome blue black R (perpendicular adsorption).

carboxylic group makes the adsorption more difficult whatever the surface. In the case of alizarin or eriochrome blue black R, besides the nature of the colorant, it must be noted that with magnetite and goethite the maximum amount of sites per nm<sup>2</sup> is close, so it is not a question of the “number” of sites but of the “nature” of sites to justify the differences.

Because of the dyes’ molecular sizes, it would be difficult to get into the iron oxide micropores from the solution, especially for the fluorescein and eriochrome blue black R dyes. Considering the Connolly molecular areas, the alizarin area is near 40 Å<sup>2</sup>, whereas fluorescein and eriochrome blue black R would be near 125 and 140 Å<sup>2</sup>, respectively. Considering a circular pore, the micropore diameters would be 19.5 Å for goethite and near 14.5 Å for magnetite and Co-goethite. Alizarin has a maximum length of near 10 Å, such as fluorescein, whereas eriochrome blue black R achieves the 13.6 Å at the maximum H–H length. These pores have microporous dimensions and are only slightly higher than the van der Waals dye molecule size, mainly for fluorescein and eriochrome blue black R. The used procedure in the iron oxides synthesis in our work is known to present reproducibility problems in terms of pore size and pore size distribution. However, the availability of the internal pores was not a main issue because of the porous size distribution of these iron oxides. We are considering mainly an external surface and the advantage of the iron oxides particle size that is characteristically low using these preparation methods. In the range of BET areas for goethite and magnetite, the reported micropore radii are not higher than 9 Å following HK and 20–30 Å following BJH when BET areas are not higher than 40 m<sup>2</sup>/g. The dye molecules used in this work are in the range of these micropore diameters, and because of molecular mobility and diffusion, it would not be easy for the dyes to get into micropores, except alizarin. The particle size is on the order of 100–140 nm, such as the literature reports.<sup>37</sup> In magnetite–water interfaces, the surface protonation states are dominated by extensive hydrolysis of interfacial water

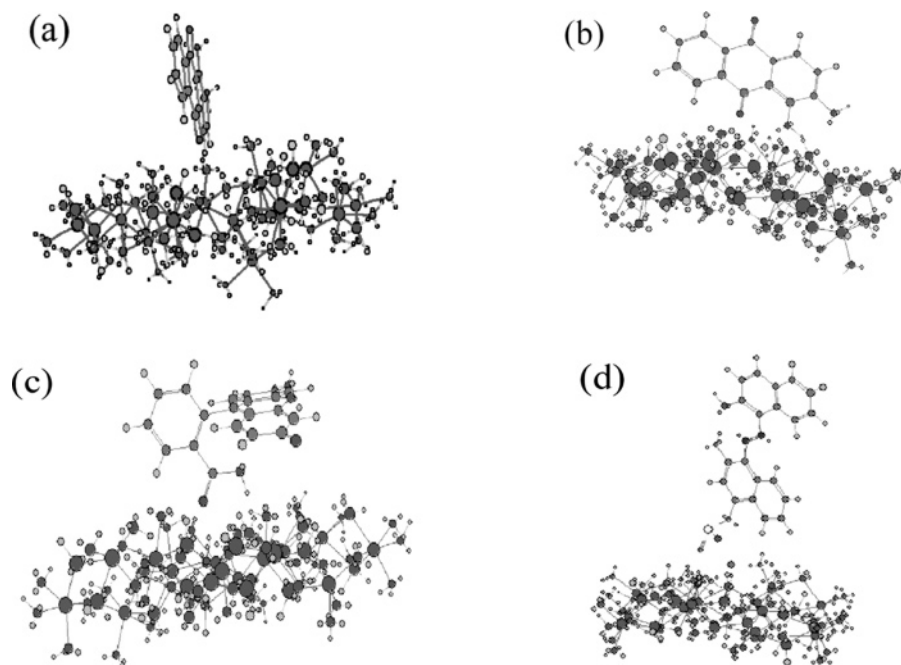
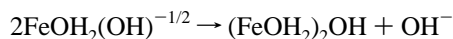


**Figure 9.** (a) Alizarin onto goethite, lateral view 1; (b) alizarin onto goethite, lateral view 2; (c) fluorescein onto goethite; (d) eriochrome blue black R onto goethite.

molecules, giving rise to a dipolar surface dominated by  $\text{FeOH}_2^+ - \text{OH}_2 - \text{OH}^-$  arrangements.<sup>38</sup> It is possible that the dominant reaction responsible for surface change development on goethite is the following reaction<sup>39</sup>



It has been reported that goethite inner sphere complexes are favored by low pH, while the relative concentrations of the outer sphere species increase with increasing pH,<sup>40</sup> while, in the case of magnetite, due to the higher charged surface of dipolar nature, different kinds of structures can be less dependent on the solution pH. These aspects will be analyzed in future work.

#### 4. Conclusions

Iron oxides were effective adsorbents to remove dyes from solution. Kinetic experiments were conducted in order to determine the equilibrium contact time. Under the conditions of the experiments all systems approached equilibrium within 90 min of contact time. All of the isotherms could be described by Langmuir and Freundlich equations. Alizarin is the dye that presents the highest affinity with the different adsorbents, while fluorescein shows the lowest affinity with the following sequence: Co-goethite > goethite > magnetite.

The MM2 modeling allowed us to consider different structures that can explain the trends found in the adsorption of the three dyes on the iron oxides studied in this work. In view of these results of alizarin adsorption on goethite and Co-goethite, the lack of the best fitting with the Langmuir isotherm can be related to the multilayer adsorption of alizarin and a possible lateral interaction of closely adsorbed alizarin molecules—as has been postulated by the MM2 calculation. Also, the surface structure in terms of surface irregularities and adsorbate lateral interactions—and therefore different adsorption enthalpies—can be related to the experimental facts.

A future work will address the effect of the pH in the adsorption process and the use of FTIR spectroscopy for the characterization of the adsorbed dyes species at the oxides surface.

#### Acknowledgment

M.L.F. and S.P. acknowledge CONICET for financial support. The authors acknowledge financial support from Universidad Nacional del Sur (Bahía Blanca, Argentina).

#### Literature Cited

- (1) Yu-Li Yeh, R.; Thomas, A. Color Difference Measurement and Color Removal from Dye Wastewaters Using Different Adsorbents. *J. Chem. Tech. Biotechnol.* **1995**, *63*, 55.
- (2) Morais, L.; Freitas, O.; Gancoloves, E.; Vaskancelos, L.; Gonzalez, C. Reactive Dyes Removal from Wastewaters by Adsorption on Eucalyptus Bark: Variables That Define the Process. *Water Res.* **1999**, *33*, 979.
- (3) Hwang, M.; Chen, K. Removal of Color from Effluents Using Polyamide-Epichlorohydrin-Cellulose Polymer II. Use in Acid Dye Removal. *J. Appl. Polym. Sci.* **1993**, *49*, 975.
- (4) Nawar, S.; Doma, H. Removal of Dyes from Effluents Using Low-Cost Agricultural By-Products. *Sci. Total Environ.* **1989**, *79*, 271.
- (5) Lee, C. K.; Low, K. S.; Gan, P. Y. Removal of Some Organic Dyes by Acid Treat Spent Bleaching Earth. *Environ. Technol.* **1999**, *20*, 99.
- (6) Kadirvelu, K.; Brasquet, C.; Cloirec, P. Removal of Cu(II), Pb(II), and Ni(II) by Adsorption onto Activated Carbon Cloths. *Langmuir* **2000**, *16*, 8404.
- (7) Kadirvelu, K.; Kavipriya, M.; Karthika, C.; Radhika, M.; Vennilamani, N.; Pattabhi, S. Utilization of Various Agricultural Wastes for Activated Carbon Preparation and Application for the Aqueous Solutions. *Bioresour. Technol.* **2003**, *87*, 129.
- (8) Jyun, T. K.; Chulhwan, P.; Eung, B. S.; Sangyong, K. Decolorization of Disperse and Reactive Dye Solutions Using Ferric Chloride. *Desalination* **2004**, *161*, 49.
- (9) Dasneshvar, N.; Aloboyeh, A.; Khataee, A. R. The Evaluation of Electrical Energy per Order for Photooxidative Decolorization of Four Textile Dye Solutions by the Kinetic Model. *Chemosphere* **2005**, *59*, 761.
- (10) Jyun, T. K.; Chulhwan, P.; Jeongmok, Y.; Sangyong, K. Comparison of Disperse and Reactive Dye Removals by Chemical Coagulation and Fenton Oxidation. *J. Hazard. Mater.* **2004**, *B112*, 95.
- (11) Bell, J.; Buckley, C. A. Treatment of Textile Dye in the Anaerobic Baffled Reactor. *Water SA* **2003**, *29*, 129.



- (12) Kapdan, I. K.; Ozturk, R. Effect of Operating Parameters on Color and COD Removal Performance of SBR, Sludge Age and Initial Dyestuff Concentration. *J. Hazard. Mater.* **2005**, *B123*, 217.
- (13) Renmin, G.; Yi, D.; Mei, L.; Chao, Y.; Huijun, L.; Yingzhi, S. Utilization of Powdered Peanut Hull as Biosorbent for Removal of Anionic Dyes from Aqueous Solution. *Dyes. Pigm.* **2005**, *64*, 187.
- (14) Herrera, F.; Lopez, A.; Mascolo, G.; Albers, P.; Kiwi, J. Catalytic Decomposition of the Reactive Dye Uniblue A on Hematite. Modelling of the Reactive Surface. *Water Res.* **2001**, *35*, 750.
- (15) Ozcan, A.; Ozcan, A. S. Adsorption of Acid Red 57 from Aqueous Solutions onto Surfactant-Modified Sepiolite. *J. Hazard. Mater.* **2005**, *B125*, 252.
- (16) Oliveira, L. C. A.; Rios, R. V. R. A.; Fabris, J. D.; Garg, V.; Sapag, K.; Lago, R. M. Activated Carbon/Iron Oxide Magnetic Composites for the Adsorption of Contaminants in Water. *Carbon* **2002**, *40*, 2177.
- (17) Allen, S. J.; Koumanova, B. Decolourisation of Water/Wastewater Using Adsorption. *J. Univ. Chem. Technol. Metal.* **2005**, *40*, 175.
- (18) Stipp, S. L. S.; Hansen, M.; Kristensen, R.; Hochella, M. F.; Bennedsen, L.; Dideriksen, K.; Balic-Zunic, T.; Léonard, D.; Mathieu, H. J. Behaviour of Fe-Oxides Relevant to Contaminant Uptake in the Environment. *Chem. Geol.* **2002**, *190*, 321.
- (19) Kosmulski, M.; Durand-Vidal, S.; Maczka, E.; Rosenholm, J. B. Morphology of Synthetic Goethite Particles. *J. Colloid Interface Sci.* **2004**, *271*, 261.
- (20) Boily, J. F.; Persson, P.; Sjöberg, S. Benzenecarboxylate Surface Complexation at the Goethite ( $\alpha$ -FeOOH)/Water Interface: III. The Influence of Particle Surface Area and the Significance of Modeling Parameters. *J. Colloid Interface Sci.* **2000**, *227*, 132.
- (21) Villalobos, M.; Trotz, M. A.; Leckie, J. A. Variability in the Goethite Surface Site Density: Evidence from Proton and Carbonate Sorption. *J. Colloid Interface Sci.* **2003**, *268*, 273.
- (22) Gaboriaud, F.; Earhardt, J. J. Effect of Different Crystal Faces on the Surface Charge of Colloidal Goethite ( $\alpha$ -FeOOH) Particles: An Experimental and Modeling Study. *Geochim. Cosmochim. Acta* **2003**, *67*, 967.
- (23) Sun, Z. X.; Su, F. W.; Forsling, W.; Samskog, P. O. Surface Characteristics of Magnetite in Aqueous Suspension. *J. Colloid Interface Sci.* **1998**, *197*, 151.
- (24) Hanna, K. Sorption of Two Aromatic Acids onto Iron Oxides: Experimental Study and Modelling. *J. Colloid Interface Sci.* **2007**, *309*, 419.
- (25) Bakoyannakis, D. N.; Deliyanni, E. A.; Zouboulis, A. I.; Matis, K. A.; Nalbandian, L.; Kehagias Th. Akaganeite and Goethite-Type Nanocrystals: Synthesis and Characterization. *Microporous Mesoporous Mater.* **2003**, *59*, 35.
- (26) Mahadevan, S.; Gnanaprakash, G.; Phillip, J.; Rao, B. P. C.; Jayakumar, T. X-Ray Diffraction Based Characterization of Magnetite Nanoparticles in Presence of Goethite and Correlation with Magnetic Properties *Physica E* **2007**, *39*, 20.
- (27) Alvarez, M.; Rueda, E.; Sileo, E. Simultaneous Incorporation of Mn and Al in the Goethite Structure. *Geochim. Cosmochim. Acta* **2007**, *71*, 1009.
- (28) Clausen, L.; Fabricius, I. BET Measurements: Outgassing of Minerals. *J. Colloid Interface Sci.* **2000**, *227*, 7.
- (29) Martell, A. E.; Smith, R. M. *Critical Stability Constants*, Vol. III; Plenum Press: New York and London, 1977.
- (30) Martell, A. E.; Smith, R. M. *Critical Stability Constants*, Vol. V; Plenum Press: New York and London, 1982.
- (31) Cañamares, M. V.; García-Ramos, J. V.; Domingo, C.; Sánchez-Cortes, S. Surface-Enhanced Raman Scattering Study of the Adsorption of the Anthraquinone Pigment Alizarin on Ag Nanoparticles. *J. Raman Spectrosc.* **2004**, *35*, 921.
- (32) Cruz, V.; Ramos, J.; Muñoz-Escalona, A.; Lafuente, P.; Peña, B.; Martínez Salazar, J. 3D-QSAR Analysis of Metallocene-Based Catalysts Used in Ethylene Polymerisation. *Polymer* **2004**, *45*, 2061.
- (33) Bygott, A. M. T.; Sargeson, A. M. Critical Evaluation of Metal Complex Molecular Mechanics. Part 1. Cobalt(III) Hexamines. *Inorg. Chem.* **1998**, *37*, 4795.
- (34) Dall'Occo, T.; Galimberti, M.; Camurati, I.; Destro, M.; Fusco, O.; Brita, D. In *Metalorganic Catalysts for Synthesis and Polymerization*; Kaminsky, W., Ed.; Springer-Verlag: Berlin, Heidelberg, Germany, 1999.
- (35) Bandara, J.; Mielczarski, J. A.; Kivi, J. I. Molecular Mechanism of Surface Recognition. Azo Dyes Degradation on Fe, Ti, and Al Oxides through Metal Sulfonate Complexes. *Langmuir* **1999**, *15*, 7670.
- (36) Başar, C. A. Applicability of Various Adsorption Models of Three Dyes Adsorption onto Activated Carbon Prepared Waste Apricot. *J. Hazard. Mater.* **2006**, *B135*, 232.
- (37) Zhang, C.; Li, S.; Wang, L.; Wu, T.; Peng, S. Studies on Decomposition of Carbon Dioxide into Carbon with Oxygen-Deficient Magnetite I. Preparation and Characterization of Magnetite and Its Activity in Decomposing Carbon Dioxide *Mater. Chem. Phys.* **2000**, *62*, 44.
- (38) Rustad, J. R.; Felmy, A. R.; Bylaska, E. J. Molecular Simulation of Magnetite-Water Interface. *Geochim. Cosmochim. Acta* **2003**, *67*, 1001.
- (39) Rustad, J. R.; Felmy, A. R.; Hay, B. P. Molecular Statics Calculations for Iron Oxide and Oxyhydroxide Minerals: Toward a Flexible Model of the Reactive Mineral-Water Interface. *Geochim. Cosmochim. Acta* **1996**, *60*, 1553.
- (40) Persson, P.; Ane, K. Adsorption of Oxalate and Malonate at the Water-Goethite Interface: Molecular Surface Speciation from IR Spectroscopy. *Geochim. Cosmochim. Acta* **2005**, *69*, 541.

Received for review February 15, 2007

Revised manuscript received September 11, 2007

Accepted September 12, 2007

IE0702476